THEORY OF RECOMBINATION PROCESSES

Christopher Bottcher
Oak Ridge National Laboratory
Oak Ridge, Tennessee 37830

(Invited paper for presentation at NATO Advanced Study Institute on "Atomic and Molecular Processes in Controlled Thermonuclear Fusion", Toulouse, France, August 13-24, 1979)

THEORY OF RECOMBINATION PROCESSES

Christopher Bottcher

Oak Ridge National Laboratory*

Oak Ridge, Tennessee 37830

§ 1. RADIATIVE RECOMBINATION

Recombination is the removal of charged particles by the association of positive and negative charges.[1] Such processes can take place in liquids and solids or on surfaces, but we confine ourselves to the gas phase. If x^+,y^- are charged bodies (small letters stand for atoms, molecules, electrons, or photons),

$$x^+ + y^- \rightarrow c \tag{1}$$

is impossible, since by time-reversal c is unstable. However,

$$x^+ + y^- \rightarrow a + b \tag{2}$$

or

$$x^+ + y^- + z \rightarrow x + y + z \tag{3}$$

are possible. The rate of disappearance of x^+ or y^- is described by the rate equations

$$\frac{dn(x^+)}{dt} = \frac{dn(y^-)}{dt} = -\alpha n(x^+)n(y^-) \tag{4}$$

*Research sponsored by the Division of Basic Energy Sciences, Department of Energy, under contract W-7405-eng-26 with the Union Carbide Corporation.

[illegible] is the recombination rate coefficient. In microscopic terms

$$\alpha(T) = \langle \sigma v \rangle \tag{5}$$

where σ is the recombination cross section, v the x-y relative velocity, and the brackets imply a Maxwell an average at temperature T.

Examples of (1) are [illegible] recombination, to which Chapters 1 and 2 are devoted, and [illegible] recombination, to which Chapter 3 is devoted. In Chapter 4 we take up *three-body recombination* defined by (3). The topics of Chapters 1 and 2 are of overwhelming importance in confined plasmas where bare or highly stripped ions predominate. Yet the topics of Chapters 3 and 4 are also important to fusion science in the design of ion sources and the production of intense neutral beams. We shall not discuss mutual neutralization,

$$x^+ + y^- \rightarrow x + y \tag{6}$$

which is sometimes classed as a recombination process.

Unless otherwise stated, we usually employ atomic units. It is convenient to list the conversions:

a.u. length a_0 = 5.2917 × 10^{-9} cm

a.u. time = 2.4189 × 10^{-17} sec

a.u. velocity = 2.1877 × 10^{8} cm sec^{-1}

speed of light = α_{fs}^{-1} (α_{fs} is the fine structure constant) in a.u.

= 137.037

1 eV = 11,605.7 deg K

1 a.u. energy = 27.21 eV = 315,790 deg K

a.u. of cross section πa_0^2 = 0.8797 × 10^{-16} cm^2

a.u. of rate $a_0^3 t_0^{-1}$ = 6.1859 × 10^{-9} cm^3 sec^{-1}

1.1. Formulae for the Radiative Rate

The simplest, and perhaps most important, recombination mechanism is single electron radiative recombination into a hydrogenic (Rydberg) orbit,

$$e + H^+ \rightarrow H(nlm) + h\nu. \tag{7}$$

Scaling to a hydrogenic ion is trivial (c.f. just below (49)). The cross section for (7) is readily derived from the Einstein A-coefficient for a transition from a continuum state, labelled by the wave-vector $\underline{k}$, to a bound state nlm,

$$\sigma_R(\underline{k},nlm) = \frac{4}{3}(2\pi a_{fs})^3 \frac{\omega^3}{k^2}\left|\langle \underline{k}|\underline{r}|nlm\rangle\right|^2. \tag{8}$$

The electron initially has energy $\epsilon = k^2/2$, while the angular frequency of the emitted photon $\omega = \epsilon + 1/(2n^2)$; $\underline{r}$ is the position vector (dipole moment) of the electron. We now replace the Coulomb wave by an expansion in eigenstates of angular momentum, average over all directions of $\underline{k}$ and sum over all states m to find

$$\sigma_R(k,nl) = \frac{8\pi^2 a_{fs}\omega^3}{3(2l+1)k^2}\left[l\langle kl-1|r|nl\rangle + (l+1)\langle kl+1|r|nl\rangle^2\right]. \tag{9}$$

The kets $|nl\rangle$, $|kl\rangle$ are associated with the radial bound and energy-normalized continuum orbitals. The rate of recombination into nl is then from (5), (9)

$$\alpha_R(nl,T) = \int_0^\infty v\,\sigma_R(v,nl)f(\epsilon,T)d\epsilon \tag{10}$$

where $v^2 = 2\epsilon$ and the Maxwellian distribution

$$f(\epsilon,T) = 2\left(\frac{\epsilon}{\pi T^3}\right)^{1/2} e^{-\epsilon/T}. \tag{11}$$

To evaluate (9), we need matrix elements of r between hydrogenic wavefunctions. Most textbooks express the wavefunctions of bound hydrogenic states as Laguerre polynomials, and of continuum states as Hypergeometric functions. These representations are not very useful for the present problem, and we turn instead to semi-classical methods which are most simply introduced through the JWKB approximation.

1.2. Radial Matrix Elements

For the n state of hydrogen the JWKB approximation[2] to the radial wavefunction is

$$g_{nl} = A_{nl}\, r^{-1}\, P^{-1/2} \sin\left(\frac{\pi}{4} + \int_{r_1}^{r} P dr\right) \tag{12}$$

where

$$P^2 = 2E_n + \frac{2}{r} - \frac{\lambda^2}{r^2},\quad E_n = \frac{-1}{2n^2},\quad \lambda = l + \frac{1}{2}, \tag{13}$$

A_{nl} is a normalization constant and r_1, r_2 are the inner, outer classical turning points. We recast P in the form

$$(nrP)^2 = n^4\epsilon^2 - (r-n^2)^2,\quad n^2\epsilon^2 = n^2 - \lambda^2 \tag{14}$$

so that ϵ is the eccentricity of the classical orbit. The substitution

$$n^2 - r = n^2\epsilon\cos z \tag{15}$$

is suggested by (14). Then the time to move on the classical orbit from perigee ($t = 0$) is given by

$$t = \int_{r_1}^{r} \frac{dr}{P} = n^3(z - \epsilon\sin z). \tag{16}$$

The azimuthal angle swept out from perigee can be obtained from conservation of angular momentum

$$r^2\frac{d\phi}{dt} = \lambda \tag{17}$$

whence

$$\phi = \lambda\int_{r_1}^{r}\frac{dr}{r^2 P} = \eta\int_0^z \frac{dz}{(1-\epsilon\cos z)},\quad \eta = \lambda/n. \tag{18}$$

Replacing z by $\zeta = \tan(z/2)$, we find that

$$\tan(\phi/2) = \frac{\eta}{(1-\epsilon)}\tan(z/2), \tag{19}$$

or equivalently

$$x = r\cos\phi = n^2(\cos\tau - \epsilon),\quad y = r\sin\phi = n^2\sqrt{1-\epsilon^2}\sin\tau. \tag{20}$$

In classical mechanics[3] τ is the eccentric anomaly, and (16), (19), and (20) define the classical motion in the (r,ϕ) or (x,y) plane.

Returning to quantal mechanics, the radial matrix elements of an operator $F(r)$ are denoted by

$$M(n\ell,n'\ell') = \langle n\ell|F|n'\ell'\rangle. \tag{21}$$

From (12) this is an integral over the product of two rapidly oscillating functions $\sin\alpha\sin\alpha'$ which we replace by $\frac{1}{2}\cos(\alpha-\alpha')$ so that

$$M(n\ell,n'\ell') = \frac{1}{2}A_{n\ell}A_{n'\ell'}\int_r^R \frac{dr}{P}\cos(a_n\Delta n + a_\ell\Delta\ell)F(r), \tag{22}$$

$$\Delta n = n-n',\quad \Delta\ell = \ell-\ell'. \tag{23}$$

The coefficients a_n, a_ℓ are given by

$$a_n = n^{-3}\int_r^R \frac{dr}{P} = n^{-3}\,t(\tau),\quad a_\ell = -\lambda\int_r^R \frac{dr}{r^2P} = -\phi(\tau) \tag{24}$$

from (16) and (18). As a special case of (22)

$$A_{n\ell} = \left[\frac{2}{\pi n^3}\right]^{1/2}, \tag{25}$$

so that for $n \gg \Delta n$, $\ell \gg \Delta\lambda$, (22) becomes

$$M(\Delta n,\Delta\ell) = \frac{\omega_o}{\pi}\int_0^\pi d\tau(\tau)F[r(\tau)]\cos[\omega_o t(\tau)\Delta n - \phi(\tau)\Delta\ell] \tag{26}$$

where ω_o is 2π/orbital period (classical) or the separation of adjacent levels (quantal).

We have derived one of a large class of results known as correspondence principles. For $\Delta n = \Delta\ell = 0$, M reduces to the expectation value of F, while (26) gives the time average of F over a classical orbit. When off-diagonal (transition) matrix elements are considered, the argument of the cosine in (26) is the difference between the classical actions in the initial and final orbits. In general, this quantity is of the form

$$\Delta(\text{action}) = \sum_j w_j(\Delta P)_j \tag{27}$$

where w_j is a canonical coordinate and ΔP_j is the change in the conjugate momentum during the transition, the sum includes a term for the pair $w = t$, $P = E$. For a dipole transition $F = r$ and $\Delta\ell = \pm 1$, so that we only have to calculate

$$M(\epsilon,\pm 1) = M_x(\epsilon) \pm iM_y(\epsilon) \tag{28}$$

where

$$M_x = \frac{\omega_o}{\pi}\int_0^\pi x\cos\theta dt,\quad M_y = \frac{\omega_o}{\pi}\int_0^\pi y\sin\theta dt,\quad \theta = \omega_o t \tag{29}$$

and x, y were defined in (20). Integrating (29) by parts (c.f. (73)), we find

$$M_x = \frac{-1}{\pi\epsilon}\int_0^\pi \sin\theta(\tau)dx(\tau),\quad M_y = \frac{i}{\pi\epsilon}\int_0^\pi \cos\theta(\tau)dy(\tau). \tag{30}$$

Inserting (20) in (30), we obtain integrals which can be expressed in terms of Bessel functions, so that[3,4,5]

$$M_x(\epsilon) = \frac{n^2}{\epsilon}J_\epsilon'(\epsilon\tau),\quad M_y(\epsilon) = \frac{n^2\sqrt{1-\epsilon^2}}{\epsilon\tau}J_\epsilon(\epsilon\tau). \tag{31}$$

We usually require the radial matrix elements squared and averaged over ℓ,

$$\begin{aligned}\mathcal{D}(n,\epsilon) &= \frac{1}{n^2}\sum_{\ell=0}^{n-1}\left[\ell M(\epsilon,-1)^2 + (\ell+1)M(\epsilon,+1)^2\right]\\ &= 2\int_0^1 \epsilon d\epsilon\,[M_x(\epsilon)^2 + M_y(\epsilon)^2].\end{aligned} \tag{32}$$

The integral over ϵ can be evaluated using the second-order differential equation satisfied by J_ϵ, with the result that

$$\mathcal{D}(n,\epsilon) = \frac{2n^4}{\epsilon^3}J_\epsilon(\epsilon)J_\epsilon'(\epsilon). \tag{33}$$

For $\epsilon \gg 1$ but still $\ll n$, we have

$$J_c(c) = \frac{0.44730}{c^{1/3}},\quad J'_c(c) = \frac{0.41085}{c^{2/3}} \tag{34}$$

whence

$$D(n,c) = \frac{2C_1 n^4}{c^6} + O(c^{-6}),\quad C_1 = 0.18377. \tag{35}$$

The asymptotic formula (35) is essentially the much-quoted Gaunt-Kramers result.[6] Even for small c, the accuracy of (34) is reasonable, as Table 1 shows. The $n \to n + c$ oscillator strength is

$$f(n \to n + c) = \frac{2c}{3n^3} D(n,c) = \frac{C_2}{2n^2}\left(\frac{n}{c}\right)^3,\quad C_2 = 0.49007. \tag{36}$$

Notice that the statistical weight of the initial level, $2n^2$, is explicitly displayed.

We now rewrite (36) in such a form that the final state n' can be extrapolated into the continuum. This will lead to the recombination cross section into n, summed over l. From (9) this total cross section is

$$\sigma_R(k,n) = 4\pi^2 a_{fc}^3 \left(\frac{n\omega}{k}\right)^2 \frac{df(n,\varepsilon)}{d\varepsilon} \tag{37}$$

where df/dε is the usual oscillator strength density *out* of the bound state,

$$\frac{df(n,\varepsilon)}{d\varepsilon} = \frac{2n}{3\pi^2} \sum_{l=0}^{\infty} \left[l\,\langle nl|r|kl-1\rangle^2 + (l+1)\,\langle nl|r|kl+1\rangle^2 \right]. \tag{38}$$

By definition the quantity $2n^2 f(n,n')$ should be symmetric in n,n' so that (36) can be written as

$$2n^2 f(n,n') = C_2 (nn'\omega)^{-3} \tag{39}$$

Table 1

c	$J_c(c)J'_c(c)$	C_1/c
1	0.14308	0.18377
2	0.07900	0.09189
3	0.05471	0.06126
4	0.04190	0.04594

Each Rydberg state n' is associated with an energy interval $d\varepsilon = (n')^{-3}$ so that (38) is equivalent to

$$2n^2 \frac{df(n,\varepsilon)}{d\varepsilon} = C_2 (n\omega)^{-3}. \tag{40}$$

The recombination cross section

$$\sigma_R(k,n) = \frac{2\pi^2}{n^3} \frac{a_{fc}^3 C_2}{\omega k^2}. \tag{41}$$

It is worth noting that the cross section for photoionizing a high n state, the inverse process to recombination, is given by[7]

$$\sigma_{PI}(n) = 4\pi^2 a_{fs} \frac{df(n,\varepsilon)}{d\varepsilon} = \frac{2\pi^2}{n^5} \frac{a_{fs} C_2}{\omega^3}. \tag{42}$$

Thus at threshold $\sigma_{PI}(n) = 16\pi$ Mb. However, the band width is proportional to the binding energy so that the total oscillator strength in the continuum

$$f_C = C_2 n^{-1}. \tag{43}$$

Most of the oscillator strength sum rule is exhausted by transitions to adjacent bound states.

1.5. Total Rates

The rate of recombination into n is obtained by inserting (41) in (10),

$$\alpha_R(n,T) = \frac{3.759 \times 10^{-6}}{n}\left(\frac{8}{\pi T^3}\right)^{1/2} \int_0^\infty \frac{k \exp(-k^2/2T)dk}{(1 + n^4 k^4)}. \tag{44}$$

Introducing the new variable $x = n^2 k^2$, we find

$$\alpha_R(n,T) = \frac{3.759 \times 10^{-6}}{n}\left(\frac{8}{\pi T}\right)^{1/2} \phi(X),\quad X = 1/(2n^2 T) \tag{45}$$

where

$$\phi(X) = Xe^X E_1(X) \tag{46}$$

and E_1 is the exponential integral.[5] As $X \to \infty$, $\phi \to 1$. In $cm^3\ sec^{-1}$, degK units the coefficient in (45) is replaced by 1.294×10^{-11}. In practice, the most needed quantities are the total rates[8]

$$a_R^{(n)}(T) = \sum_{m=n}^{\infty} a_R(m,T) \tag{47}$$

where $n = 1,2$ for plasmas which are optically thin, thick in the Lyman-α line. Thus, we write

$$a_R^{(n)}(T) = \frac{2.065 \times 10^{-11}\ cm^3\ sec^{-1}}{(T\ degK)^{3/2}}\ \phi_n(X_1) \tag{48}$$

where

$$\phi_n(X_1) = \sum_{m=n}^{\infty} \frac{1}{m}\phi\left(\frac{X_1}{m^2}\right),\quad X_1 = \frac{1.5789 \times 10^5}{T\ degK}. \tag{49}$$

Figure 1 shows the variation of ϕ_1, ϕ_2 with X_1. For a hydrogenic ion of nuclear charge q, (48) is multiplied by q^2. It appears from (45) that the favored values of n are those for which $2n^2T \sim 1$. The asymptotic formulae (41), etc. should not be used for $T \gg 3 \times 10^5$ q^2 degK.

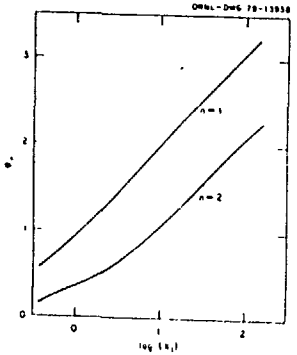

Fig. 1. Variation of functions ϕ_1, ϕ_2 defined in (49).

1.4. Partial Rates

We now turn to the more recondite question of the distribution among ℓ-substates. This is often not of practical importance since the ℓ-s will be statistically redistributed following a single collision with a charged particle. However, in an intense radiation field, low-ℓ states are preferentially photoionized, and since recombination favors just these states, the assumption of redistribution would overestimate the number of neutrals. The dependence of the rates on ℓ was first discussed in detail by Burgess.[9] A convenient table for n-1, $\ell \le 11$ and T = 1 eV is given in Ref. 1.

First, consider how the bound-bound matrix elements (28) - (31) depend on ℓ. In Fig. 2 we plot $\mu_\pm$ vs. ϵ for $\epsilon \le 4$, where

$$M(\epsilon,\ell 1) = n^2\ \mu_\pm(\epsilon). \tag{50}$$

These numbers were generated by evaluating (26) numerically. Using asymptotic formulae for the Bessel functions (31), we find that

$$|\mu_+|^2 + |\mu_-|^2 = \frac{\pi S^{2\epsilon}}{n\epsilon^2\Gamma^2},\quad S = \frac{4e^n}{1+n}\ (1-\epsilon > 1/8\ \epsilon^{2/3}). \tag{51}$$

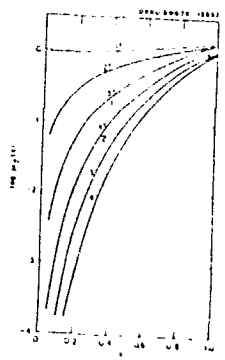

Fig. 2. Variation of $\mu_\pm(\epsilon)$, defined by (26) and (50), with ϵ. Notice that $\mu_+(\epsilon) = \mu_-(\epsilon-2)$.

The accurate calculations and asymptotic formulae agree that, except for $\mu_\ell(1)$, all the matrix elements $\to 0$ rapidly as $\varepsilon \to 0$, i.e., as the classical orbits become circular. It is not possible to extrapolate (51) into the continuum, though it correctly suggests that very low ℓ-s are favored.

We can rewrite (9) in terms of either velocity or acceleration matrix elements. For exact eigenstates,

$$\begin{aligned} \langle i|\underline{r}|f\rangle &= (i\omega)^{-1} \langle i|\underline{p}|f\rangle \text{ (velocity)} \\ &= (i\omega)^{-2} \langle i|\underline{r}/r^3|f\rangle \text{ (acceleration).} \end{aligned} \tag{52}$$

Then the dipole matrix elements in (9) can be replaced by

$$I_\ell(n,k\ell) = \langle n\ell|r^{-2}|k\ell\pm1\rangle \tag{53}$$

times ω^{-2}. Since the acceleration matrix element weighs the region of space near the nucleus, it is possible to replace the high-n orbital by a continuum orbital of zero energy

$$\lim_{n\to\infty} n^{3/2} \langle r|n\ell\rangle = \lim_{k\to 0} \langle r|k\ell\rangle \tag{54}$$

when $|k\ell\rangle$ is energy normalized. Then (53) becomes

$$I_\ell(n,k\ell) = n^{-3/2} J_\ell(k\ell),\ J_\ell(k\ell) = \langle n\ell|r^{-2}|o\ell\pm1\rangle \tag{55}$$

while the recombination cross section

$$\sigma_R(k,n\ell) = \frac{8\pi^2}{3n^3}\frac{\alpha_{fs}^2}{\omega k^2} S_\ell(k) \tag{56}$$

$$S_\ell(k) = \frac{1}{(2\ell+1)} [\ell J_-(k\ell)^2 + (\ell+1)J_+(k\ell)^2]. \tag{57}$$

This is equivalent to (41) if

$$\sum (2\ell+1)S_\ell(k) = S(k) \tag{58}$$

is constant and close to $2C_1$ over a reasonable range of k. This is verified to be so by direct numerical calculation (Fig. 3). In Fig. 4 we show histograms of

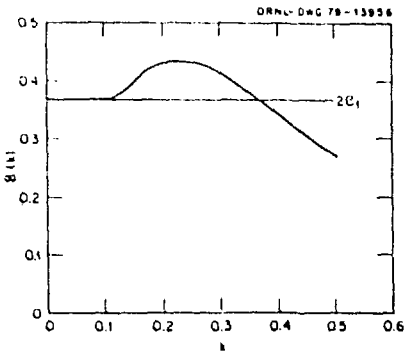

Fig. 3. Variation of S(k) defined by (57), (58) with k.

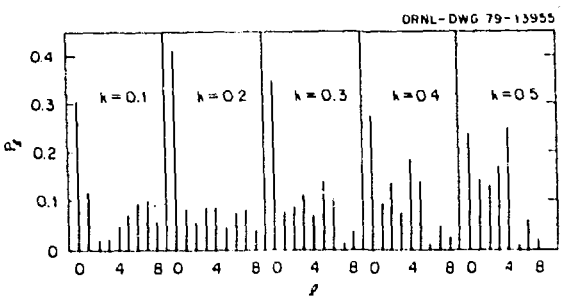

Fig. 4. Histograms of P_ℓ, the distributions defined in (59).

$$P_\ell = (2\ell+1)S_\ell(k)/S(k) \tag{59}$$

which represent the distribution over ℓ for different initial energies. As is well known, $S_\ell(k)$ oscillates as a function of ℓ and k, but this structure does not persist in the rates. Most recombination is into states $\ell \sim k$. In Fig. 5 we show the rates into all n of a given ℓ,

$$\alpha_R^*(\ell,T) = \sum_{n=\ell+1}^{\infty} \alpha_R(n,T) \tag{60}$$

for several ℓ, compared with the total, $\alpha_R^{(1)}$ of (48).

Burgess used the different approach of extracting the approximate analytic dependence on k from the length matrix elements, so that

$$\omega^{-2}\, I_\ell(n,k\ell) = n^2\, B_\ell(n\ell) \left(\frac{\omega}{\omega_n}\right)^{S_\ell(k)}, \tag{61}$$

$$\omega_n = 1/(2n^2),\quad n^2\, B_\ell(n\ell) = \langle n\ell|r|0k\pm1\rangle.$$

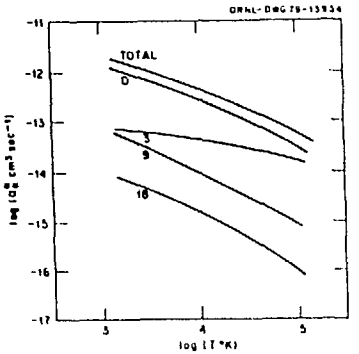

Fig. 5. $\alpha_R^*(\ell,T)$ as defined in (60), vs. T. The total rate into all bound states is also shown.

The functions $B_\ell = \omega B_\ell$ and $S_\ell = S_\ell/n^2$ are tabulated[9] for $\ell \le n-1 \le 11$. This representation is valid for $\omega < \omega_n$. Typical values of B_ℓ are ~ 2.0, while $B_1 \sim 1.5$, $B_- \sim 0.3$. However, B_ℓ increases with ℓ, and B_ℓ have a slow variation with n,ℓ such that

$$\sum_{\ell=0}^{n-1} [\ell B_-(n\ell)^2 + (\ell+1)B_+(n\ell)^2] \approx 2.n. \tag{62}$$

We now rewrite (61) as

$$I_\ell(n,k\ell)^2 = \left(\frac{\omega}{\omega_n}\right)^{2S_\ell(k)} \frac{B_\ell(n\ell)^2}{[2n^2]^2} \tag{63}$$

and insert in (62). Taking $n \sim k$, which overestimates the contribution of large ℓ, (62) leads back to (41) with $2C_1$ replaced by 0.55. The variation of B_ℓ with ℓ is such that low ℓ-s are highly favored, as we should expect.

§ 2. DIELECTRONIC RECOMBINATION

2.1. Introduction

In Chapter 1 we saw that single electron radiative recombination falls off reasonably rapidly with the energy of the free electron, simply because the matrix element connecting the free and bound states must decrease as the deBroglie wavelength $2\pi/k$ decreases, (41). If, however, the recombining ion is not a bare nucleus, the incident electron can be slowed by exciting some of the bound electrons. Following this line of thought, one is led to consider *dielectronic recombination* (DIR),

$$e(k\ell) + A^{+q}(\alpha) \rightleftarrows A^{+q-1}(\beta,n\ell') \tag{64a}$$

$$\rightarrow A^{+q-1}(\gamma,n\ell') + h\nu \tag{64b}$$

where $\beta \to \gamma$ is an allowed dipole transition of A^{+q}. Often $\gamma = \alpha$ = ground state, but γ,α may be distinct excited states. In the first stage of (64) the original ion is excited sufficiently that the electron is captured into a high hydberg state (Fig. 6). This state is unstable in that it may autoionize back to the initial, or some other, channel. Recombination is achieved if the excited core†

† By "core" we always mean A^{+q}, the core of A^{+q-1}. It is not implied that inner shells of A^{+q} are excited, though they might be.

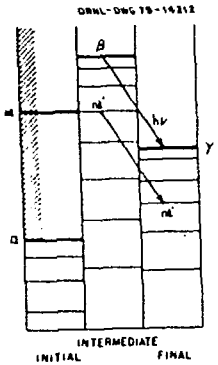

Fig. 6. Scheme of dielectronic recombination (64).

decays radiatively to produce a stable state (we shall not consider the complication that it could produce another unstable state). Typically, the radiative lifetime ~ 10^{-10} sec, while the radiationless lifetime ~ $3 \times 10^{-16}\ n^3$ sec, so that radiative decay (stabilization) is more likely for $n > n_0 \sim 70$. For a given electron in the bandwidth of the Rydberg series, the probability of being in a resonance[1] is ~ 50%, while the probability that the resonance stabilizes is ~ 100% ($n > n_0$) or the ratio of the lifetimes ($n < n_0$), whence the probability of stabilization

$$P_n = 0.5\ \mathrm{MIN}\ [1,\ (n/n_0)^3] \tag{65}$$

where nℓ' is the Rydberg state nearest in energy. Averaging (65) over energy (multiply P_n by q^2/n^3, sum over n and divide by $q^2/2$) we arrive at a mean probability

$$P = 1/n_0^2. \tag{66}$$

[1] The autoionizing states are resonances in the electron scattering channel.

If the bulk of the Maxwellian overlaps the Rydberg series and the electronic temperature ~ 10^5 deg K, P is just the rate in a.u.

$$\alpha_{DIR} = 10^{-12}\ N\ \mathrm{cm}^3\ \mathrm{sec}^{-1} \tag{67}$$

where N is the number of Rydberg series (β,ℓ'). In the most favorable cases, α_{DIR} reaches a few times 10^{-11} cm^3 sec^{-1}. Since the radiative rate at $T = 3 \times 10^5$ degK is $\alpha_R = 3 \times 10^{-14}\ q^2$ cm^3 sec^{-1}, dielectronic recombination dominates wherever core transitions α → β are readily excited (at least for q < 20). We shall see that α_{DIR} has an intricate dependence on charge state, temperature, and species, though the range of values spanned is usually limited to 10^{-12} - 10^{-11} cm^3 sec^{-1}.

The process (64) was first suggested in the 1930's but early discussions only considered a single autoionizing state thus underestimating the rate by a factor ~ n_0. In the early 1960's discrepancies in the temperature of the solar corona derived from ionization equilibrium theory and that derived from direct measurements of Doppler widths led to the search for a missing recombination process. By considering an entire Rydberg series, Burgess[11] arrived at DIR rates large enough to explain the coronal equilibrium. Notable contributions were also made by Shore[12] and McCarroll.[13] In these lectures we can only present a rather simplified introduction to the problem. For more information, the recent excellent review by Seaton and Storey[14] should be consulted.

2.2. Formal Theory

Since we are not here concerned with scattering theory as such, we shall simply quote the standard result of resonant scattering theory with many channels.[10] For a series of well-separated resonances n, decaying into channels i, the cross section i → j is given by

$$\sigma_{ij} = \sum_\ell (2\ell+1)\sigma_{ij}(\ell),\ \sigma_{ij}(\ell) = \frac{\pi}{k_i^2} \sum_n \frac{\Gamma_{ni}\,\Gamma_{nj}}{(\epsilon-\epsilon_n)^2 + \Gamma_n^2/4} \tag{68}$$

where ℓ is the total angular momentum and k_i the initial wavenumber. Each resonance has position ϵ_n, partial widths Γ_{ni} and total width (also rate of decay in a.u.)

$$\Gamma_n = \sum_j \Gamma_{nj} \tag{69}$$

in general depending on ℓ. The meaning of (68) is clear: each resonance has the overall Breit Wigner energy dependence, while the

branching ratios for different processes are proportional to the products of the entrance and exit partial widths.

It is straightforward to apply (68) to (64). For a single pair of angular momenta ℓ,ℓ'

$$\sigma_{DIR}(\ell,\ell') = \frac{\pi}{k^2}\sum_n \frac{\Gamma_a(\beta,n\ell';\alpha,\ell)\Gamma_r(\beta,n\ell';\gamma)}{(\epsilon-\epsilon_n)^2+\Gamma(\beta,n\ell')^2/4} \tag{70}$$

where the subscripts r,a refer to radiative and autoionizing decays. Though angular momentum couplings are not explicitly shown in (70), it is necessary to sum over all initial, intermediate, and final substates, finally dividing by the statistical weight of α. The total width

$$\Gamma(\beta,n\ell') = \sum_{\alpha'\ell} \Gamma_a(\beta,n\ell';\alpha',\ell) + \sum_{\gamma'} \Gamma_r(\beta,n\ell';\gamma'). \tag{71}$$

Certain simplifying assumptions are made:

(i) the resonances are narrow compared with their spacing;

(ii) the energy levels ϵ_n do not depend on ℓ', i.e. quantum defects are small;

(iii) only the decay channels $\alpha' = \alpha$, $\gamma' = \gamma$ are significant,

(iv) the radiative decay rate is independent of $n\ell'$ and is simply the A-coefficient for $\beta \to \gamma$ in A^{+q}.

If we write

$$\Gamma_a(n\ell') = \sum_\ell (2\ell+1)\Gamma_a(\beta,n\ell';\alpha,\ell),\quad \Gamma(n\ell') = \Gamma_r + \Gamma_a(n\ell') \tag{72}$$

for ϵ_n and sum (70) over ℓ, the contribution from a single Rydberg series (β,ℓ') becomes

$$\sigma_{DIR}(\ell') = \frac{\pi}{k^2}\sum_n \frac{\Gamma_a(n\ell')\Gamma_r}{(\epsilon-\epsilon_n)^2+\Gamma(n\ell')^2/4}. \tag{73}$$

To obtain a rate from (73), we must evaluate

$$\alpha_{DIR}(\ell') = \left(\frac{2}{\pi T^3}\right)^{1/2}\int_0^\infty k^2\,\sigma_{DIR}(\ell')\exp\left(-\frac{\epsilon}{T}\right)d\epsilon. \tag{74}$$

Replacing

$$\frac{\Gamma_a\Gamma_r}{(\epsilon-\epsilon_n)^2+\Gamma^2/4} \to \frac{2\pi\Gamma_a\Gamma_r}{\Gamma}\,\delta(\epsilon-\epsilon_n),$$

we find from (73) and (74) that

$$\alpha_{DIR}(\ell') = \left(\frac{\pi}{T}\right)^{3/2}\sum_n \frac{\Gamma_a(n\ell')}{\Gamma(n\ell')}\frac{\Gamma_r}{\Gamma_r}\exp\left(-\frac{\epsilon_n}{T}\right). \tag{75}$$

The energy levels must be referred to the initial state of A^{+q}. All discussions of DIR are based on (76).

2.3 Calculation of Rates

The decay process (6b,a) is closely related to the excitation process

$$e(k\ell) + A^{+q}(\alpha) \to e(k'\ell') + A'^{+q}(\beta). \tag{76}$$

The threshold cross section ($k' \to 0$) and widths ($n \to \infty$) can be written in terms of the same functions $G_a(k\ell,k'\ell')$,

$$\sigma_{ex}(k) = \frac{\pi}{k^2}\sum_{\ell\ell'}(2\ell+1)G_a(k\ell,k'\ell'), \tag{77a}$$

$$\Gamma_a(n\ell') = n^{-3}\sum_\ell (2\ell+1)G_a(k_0\ell,0\ell'), \tag{77b}$$

where $k_0^2/2$ is the threshold energy. Henceforth we write $G_a(k_0\ell,0\ell') = G_a(\ell')$. We shall presently calculate G_a in the Coulomb-Born-Dipole approximation, but first (75) can be developed further.

It will turn out that G_a is insensitive to q, while Γ_r varies strongly,

$$\Gamma_r = \frac{4}{3}\alpha f_{\beta\gamma}\omega^3|\langle\beta|\underline{D}|\gamma\rangle|^2. \tag{78}$$

The dipole operator of A^{+q} is $\underline{D}$; (78) implies summation over the substates of γ and averaging over the substate of β. The dipole matrix element $\sim q^{-1}$, while

$$\omega = E_\beta - E_\gamma = G\,q^{\mu+1} \tag{79}$$

where $\mu = 0,1$ if the principle quantum number changes by

$|N_\beta - N_\gamma| = 0, \geq 1$ so that

$$\Gamma_r = G_r\, q^{3\mu+1}. \tag{80}$$

Inserting (77b), (80) in (75) we see that a key role is played by the principal quantum number n_c for which $\Gamma_r = \Gamma_a$,

$$n_c(\ell') = \left(\frac{G_a}{\Gamma_r}\right)^{1/3} = \left(\frac{G_a}{G_r}\right)^{1/3} q^{-\mu-\frac{1}{3}}. \tag{81}$$

Then the rate is given by

$$a_{DIR}(\ell') = \Gamma_r \sum_n \frac{F(\epsilon_n,T)}{[1+(n/n_c)^3]},\ F(\epsilon,T) = \left(\frac{2\pi}{T}\right)^{3/2} e^{-\epsilon/T}. \tag{82}$$

Most of the sum comes from high values of n for which $\epsilon_n = \omega$ (if $\gamma = a$ for simplicity). Then (82) becomes

$$a_{DIR}(\ell') = 1.21\ \Gamma_r\ n_c(\ell')F(\omega,T), \tag{83}$$

and on using (80),

$$a_{DIR}(\ell') = 1.21\ G_{ra}(\ell')q^{2\mu+\frac{2}{3}} F(\omega,T),\ G_{ra}(\ell') = [G_r^2 G_a(\ell')]^{1/3}. \tag{84}$$

The total rate is obtained on summing over ℓ' (the sum over substates of ℓ' is already contained in G_a),

$$a_{DIR} = 1.21\ G_{ra}\, q^{2\mu+\frac{2}{3}} F(\omega,T),\ G_{ra} = \sum G_{ra}(\ell'). \tag{85}$$

This function peaks at $T = \frac{2}{3}\omega$, as one might have expected, the maximum value being

$$a_{DIR-MAX} = 6.37\ G_{ra}\, G^{-3/2}\ q^{\frac{1}{2}\mu-\frac{5}{6}}. \tag{86}$$

i.e. for $\mu = 0$, $a_{DIR-MAX} \sim q^{-5/6}$ and for $\mu = 1$, $\sim q^{-1/3}$. Thus, in Saha equilibrium $\mu = 1$ transitions are more important.

Before calculating G_a, we must digress on angular momentum coupling. The state β is usually specified by Russell-Sanders quantum numbers $S_\beta L_\beta J_\beta$, while the outer electron couples to J, giving a total angular momentum K. The full set of quantum numbers is $(\beta S_\beta L_\beta J, n\ell', KM_K)$. If we average over JKM_K and ignore the small differences in energy between different JK states, the result is as if we had used an uncoupled representation and averaged over the magnetic quantum numbers $(\beta L_\beta M, n\ell' m')$. This procedure should be good except in some small energy ranges which do not significantly affect the rate. Then the autoionization width is given by the "golden rule",

$$G_a(\ell') = 2\pi q^2 \sum |\langle \beta L_\beta M', \alpha\ell' m'|V|\alpha L_\alpha M, k_c \ell m\rangle|^2, \tag{87}$$

where we sum over M, and average over M'm'. The interaction

$$V = \sum |\underline{r}-\underline{r}_j|^{-1} \tag{88a}$$

where $\underline{r}$ is the position of the outer electron and j runs over the electrons of A^{+q}. To evaluate (87) we retain only the dipole term

$$V = \underline{D}\cdot\underline{r}/r^3 \tag{88b}$$

whence

$$G_a(\ell') = 2\pi q^2 \sum_\ell c(\ell\ell')(L_\alpha 1 L_\beta)R(\alpha,\beta)^2\, J(\ell,\ell')^2. \tag{89}$$

The angular integral

$$c(\ell\ell') = \mathrm{MAX}(\ell,\ell') \tag{90}$$

J is the same integral introduced in (55),

$$J(\ell,\ell') = \langle k_c \ell|r^{-2}|\alpha\ell'\rangle \tag{91}$$

and R is the radial integral (for a one-electron transition -- more generally it is a reduced matrix element),

$$R(\alpha,\beta) = \langle\alpha|r|\beta\rangle. \tag{92}$$

Since Γ_r is also proportional to R^2, we can express (89) in the form

$$\frac{G_a(\ell')}{\Gamma_r} = \frac{1.17\times 10^7}{\omega^3 q^2}\,[\ell' J(\ell'-1,\ell')^2 + (\ell'+1)J(\ell'+1,\ell')^2]. \tag{93}$$

It is interesting that according to (93) the radiationless process (64a) is related to radiative recombination via the acceleration matrix elements. The integral (91) can be scaled to $q = 1$,

$$J(\ell,\ell'|k_o,q) = J(\ell,\ell'|k_o/q,1). \tag{94}$$

Since $R \sim q^{-1}$, an immediate consequence is that $G_a \sim q^0$, as stated above. Then (93) becomes

$$G_a(\ell') = 1.217 \times 10^7 \frac{\Gamma_r q^2}{\omega^3} T(\ell') \tag{95}$$

where $T(\ell) = (2\ell+1)S_\ell(k_o/q)$, and S_ℓ was defined in (57). From Fig. 4 we see that G_a must fall off rapidly when $\ell' > 5$. From (79), (80), (84), (85), and (95),

$$G_{rR} = 230\, C_3\, G^{-1}\, G_r \quad , \quad C_3 = \sum_\ell T(\ell)^{1/3} = 2.0 (k_o < q). \tag{96}$$

Then the total rate

$$\alpha_{DIR} = 278\, C_3 q^{2\mu} + \tfrac{2}{3} G^{-1}\, G_r F(\omega,T). \tag{97}$$

Finally, the peak rate

$$\alpha_{DIR-MAX} = 1470\, C_3 q^{\frac{1}{2}\mu - \frac{5}{6}} G^{-5/2}\, G_r. \tag{98}$$

To illustrate the zoology of autoionizing states, we look in detail at a series in four-electron ions

$$A^{+q-1}(1s^2\, 2pnp) + A^{+q}(1s^2\, 2s) + e(ks,kd) \tag{99}$$

which is strongly excited in ion-atom collisions.[15] Thus $\alpha = 2s$, $\beta = 2p$, $\ell' = 1$, $\ell = 0,2$; in (79), $\mu = 0$. Table 2 shows the variation with q of ω/q, qR, $J(p\to s)$ and $J(p\to d)$: ω, $R(2s\to 2p)$ are the best experimental and theoretical values[16] and J was calculated with Coulomb wavefunctions. The regularity of scaling with q is pleasing From (89) we obtain the reduced widths

$$G_a = 2\pi\, (qR)^2\, [J(p\to s)^2 + 2J(p\to d)^2]. \tag{100}$$

Table 2 shows the *average* width of one multiplet (2pnp)SL, $\frac{1}{9} G_a$. The perturbation theory is valid[10] if $\frac{1}{9} G_a < 2\pi$ which is just about satisfied. Because of the resonance oscillator strength, these widths are unusually large, e.g. in his study of He-like systems, Weisheit[17] used the universal formula

$$G_a(\ell') = 1.6 \times 10^{-5}\, (2\ell'+1) \quad (\ell' \le 7)$$
$$= 0 \qquad\qquad\qquad\quad (\ell' > 7). \tag{101}$$

Table 2. Variation with q of matrix elements entering DIR

q	1	2	3	5	8	16
$10\,\omega/q$	0.680	0.728	0.735	0.736	0.740	0.779
qR	7.06	7.90	8.20	8.48	8.67	8.76
$J(p\to s)$	0.0829	0.132	0.154	0.169	0.172	0.166
$J(p\to d)$	0.0205	0.0411	0.0514	0.0580	0.0602	0.0674
$\frac{1}{9} G_a$	0.268	0.906	1.36	1.77	1.96	1.96

All quantities refer to the process (99) - (103).

However, G_r is compensatingly small because of the ω^3 factor. Using the values at $q = 8$, $G = 0.074$ and $G_r = 5.26 \times 10^{-9}$, so that $G_{rR}(1) = 7.87 \times 10^{-6}$ and the total $G_{rR} = 3.27 \times 10^{-5}$. From (97) the total rate is

$$\alpha_{DIR} = (2.42 \times 10^{-11}\ \mathrm{cm}^3\ \mathrm{sec}^{-1}) q^{0.67}\, F(0.074q,T) \tag{102}$$

of which $\ell' = 1$ contributes 24%. The maximum rate (at T = 15,600 q degK) is

$$\alpha_{DIR-MAX} = (6.34 \times 10^{-11}\ \mathrm{cm}^3\ \mathrm{sec}^{-1}) q^{-0.83}. \tag{103}$$

The chief defect of (89) - (98), which are intended as illustrations rather than working formulae, is the Coulomb approximation in evaluating J. If distorted waves are used for $q > 3$, the results would probably be as good as one could desire; for $q \le 3$ close-coupling calculations might be needed. Referring to (84), α_{DIR} depends on G_a, which must be calculated, only through the one-third power; G_r is usually available in the large body of critically assessed oscillator strengths. If (98) is applied to the He^+ sequence, $G_{rR} = 7.44 \times 10^{-5}$ and $\alpha_{DIR-MAX} = (1.59 \times 10^{-12}\ \mathrm{cm}^3\ \mathrm{sec}^{-1}) q^{-0.33}$, in good agreement with the best calculation;[18] 20% comes from the 2pnp series. For most applications, the semi-empirical universal formula of Burgess[11] is recommended.

In Fig. 7 we show the best available calculations[14,18] of α_{DIR} for He^+, C^{+2}, and Fe^{+21} compared in each case with the radiative rate α_R. The core transition in He^+ has $\mu = 1$ (1s→2p) and that in C^{+2} has $\mu = 0$ (2s→2p); in Fe^{+21} two transitions contribute, one $\mu = 0$ (2s→2p) and one $\mu = 1$ (2p→3d). Since α_{DIR} falls off with q, albeit slowly, and $\alpha_R \sim q^2$, the latter eventually catches up, as can be seen in Fe^{+21}.

Though outside the scope of these lectures, collisions with third bodies may have an important effect on DIR. In dense plasmas

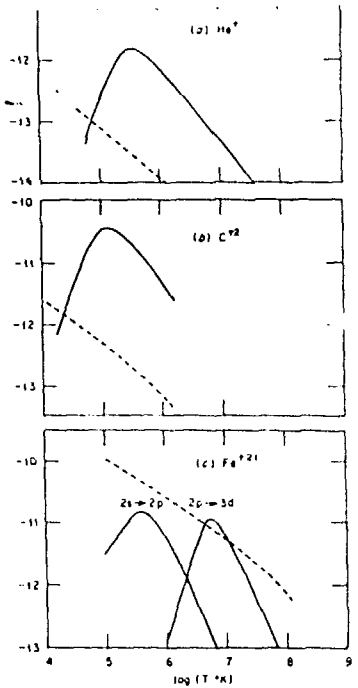

Fig. 7. Variation of DIR rate with temperature. The full lines are α_{DIR} and the dotted lines are α_R. Two transitions contribute in Fe^{+21} as indicated. The results for He^+ are from close-coupling[18] and for C^{+2}, Fe^{+21} from distorted-wave calculations.[14]

ionization, large values of ℓ' are populated, thereby stabilizing the state.

§ 3. DISSOCIATIVE RECOMBINATION

3.1. Introduction

Dissociative recombination (DR) is the process suggested by Bates and Massey in 1947 to account for the removal of O_2^+ in the ionosphere,

$$e + AB^+ \rightarrow A(n) + B(n.) \qquad (1.4)$$

where one or both products is usually excited. The process is important at temperatures below 1 eV where molecular ions are abundant. Its rapid rate is explicable if the dissociating state of AB crosses the ionic state in the Franck-Condon (FC) region of the ground vibrational state (Fig. 8). For most systems with more than four electrons, one can almost always find an electronically doubly excited surface AB^{**} satisfying this requirement. The few electron systems of special interest in neutral beam technology provide exceptions to this rule. Accurate potential energy curves[19] for $H_2^+(1s_g)$ and $H_2(1s_g^2\ {}^1\Sigma_g^+)$ are shown in Fig. 9. The crossing point R_x lies within the FC region for initial vibrational states $v \geq 3$. In H_3^+ a similar situation prevails;[20] at least 0.5 eV of excitation is required to reach the lowest dissociating surface from the ground vibrational state. The only molecular ion for which dissociative recombination is never significant may be He_2^+. The molecular orbitals $1s_g$, $1s_u$ based on 1s atomic orbitals are fully occupied in ground state He_2; thus, the lowest doubly excited state involves two orbitals based on 2s,2p atomic states and lies ~ 16 eV above the ionic ground state (relative to $2He^+$, $He + He^+$ ~ -26 eV, while $He_2^{**} \rightarrow 2He^*$ ~ -10 eV).

3.2. Formalism

The formal theory of (1.4) is an interesting problem on which a large literature has accumulated.[19,20] We only present a simplified account here, confined to diatomics for the most part. Rather than consider the crossing state as the final (adiabatic) channel, we define it to be a diabatic state which crosses the true final state, as illustrated in Fig. 8.

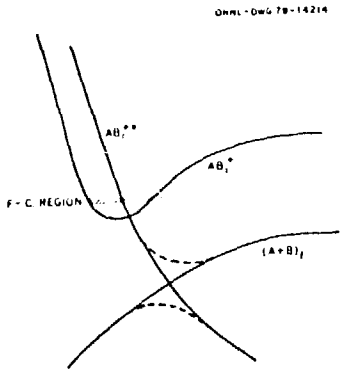

Fig. 8. Scheme of dissociative recombination (104), (105).

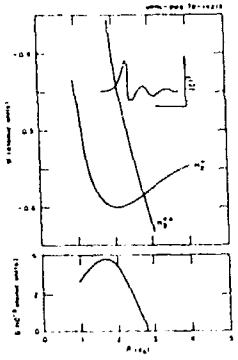

Fig. 9. Accurate potential energy curves[19] for $H_2^+(1s\sigma_u)$ and $H_2^{**}(1s\sigma_u^2)$. Inset are the width G of the H_2^{**} data and the squared nuclear wavefunction $|\zeta|^2$ of the dissociating state H + H* (c.f. (119)).

$$e(\varepsilon) + AB_1^+ \ddagger AB_r^{**} \rightarrow (A+B)_f \tag{105}$$

The born-oppenheimer electronic wavefunctions at given internuclear separation R of the three states in (105) are denoted by $\phi_1(\varepsilon)$, ϕ_r, ϕ_f. In the first place, we suppose that the incoming electron has energy $\varepsilon_1 = k_1^2/2$, total angular momentum L_1 and projected angular momentum on the internuclear axis λ_1. The rotation of the ion is ignored as is permissible at energies $\varepsilon_1 \gg$ rotational separations. It is vital to realize that AB^{**} can decay by ejecting electrons of energy $\varepsilon \neq \varepsilon_1$, the slack being taken up by the nuclear (vibrational) motion. Much of the literature is concerned with the definition of the resonance state ϕ_r which we take as intuitively known. The electronic-vibrational wavefunction of the system (105) can be expanded as

$$\Psi(L_1\lambda_1) = F_f(R)\phi_f + F_r(R)\phi_r + \int d\varepsilon\, F_1(\varepsilon,R)\phi_1(\varepsilon). \tag{106}$$

If the potentials are $\varepsilon + W_1$, W_r, W_f and the diabatic couplings are $V_{r1}(\varepsilon)$, V_{rf}, we obtain the following set of coupled equations,

$$(E-K-W_f)F_f = V_{fr}F_r \tag{107}$$

$$(E-\varepsilon-K-W_1)F_1(\varepsilon) = V_{1r}(\varepsilon)F_r \tag{108}$$

$$(E-K-W_r)F_r = V_{rf}F_f + \int d\varepsilon\, V_{r1}(\varepsilon)F_1(\varepsilon) \tag{109}$$

where E is the total (electronic plus vibrational) energy and K the nuclear kinetic energy operator (M is the reduced mass)

$$K = -\frac{1}{2MR^2}\frac{\partial}{\partial R}\left[R^2\frac{\partial}{\partial R}\right]. \tag{110}$$

If $V_{r1}(\varepsilon)$ varies slowly with R and F_r is approximately an eigenstate of $K+W_r$, i.e. if the right side of (109) is neglected to a first approximation, (108) has a particular integral equal to F_r times a slowly varying function of R. To this integral must be added a solution of the homogeneous equation

$$(E-\varepsilon_1-K-W_1)\zeta_1 = 0 \tag{111}$$

to provide an ingoing wave in (108). Thus

$$F_1(\varepsilon) = \zeta_1\delta(\varepsilon-\varepsilon_1) + (\varepsilon_{r1} - \varepsilon + i0)^{-1}V_{r1}(\varepsilon)F_r \tag{112}$$

where

$$\epsilon_{ri}(R) = W_r - W_i \tag{113}$$

is the "vertical ejection energy". If AB was in the state r with the nuclei fixed at R, it would autoionize to AB^+ by ejecting an electron of energy $\epsilon_{ri}(R)$. The positive imaginary term in the denominator of (112) insures that only outgoing waves appear in the final channel. Substituting (112) in (109), we find that

$$(E-K-W_r)F_r = V_{ri}(\epsilon_i)\zeta_i + V_{rf}F_f + \mathcal{D}F_r \tag{114}$$

where

$$\mathcal{D} = \int \frac{V_{ri}(\epsilon)^2\, d\epsilon}{\epsilon_{ri}-\epsilon+i0} = \frac{i}{2}G_r,\quad G_r = 2\pi V_{ri}(\epsilon_{ri})^2 \tag{115}$$

neglecting a principal value integral. The "vertical" or "local" width G_r is now incorporated in a complex potential

$$W_r = W_r - \tfrac{i}{2}G_r \tag{116}$$

so that

$$(E-K-W_r)F_r = V_{ri}(\epsilon_i)\zeta_i + V_{rf}F_f. \tag{117}$$

Solution of (107) and (117) leads to the amplitude of the outgoing wave in F_f and hence to the DR cross section. Generalization to many final states is obvious. Back ionization into the initial state is described by the complex potential W_r.

To calculate the cross section, we return to the representation in which W_r crosses W_f so that r is itself the final channel, and V_{rf} is dropped from the right side of (117). It is readily shown from Green's theorem that as $R \to \infty$,

$$F_r \to A(\ell_i\lambda_i,\epsilon_i)\left(\frac{2\pi M}{k_f}\right)^{1/2}\frac{e^{ikR}}{iR},$$
$$A(\ell_i\lambda_i,\epsilon_i) = \langle\zeta_r|V_{ri}(\epsilon_i)|\zeta_i(\epsilon_i)\rangle \tag{118}$$

where ζ_r is a solution of the homogeneous equation

$$(E-K-W_r)\zeta_r = 0 \tag{119}$$

so normalized that

$$\zeta_r \to \left(\frac{2M}{\pi k_r}\right)^{1/2}\frac{\sin\eta}{R}\ ,\quad \eta = k_rR + \delta_r \tag{120}$$

where δ_r is a complex phase shift. To obtain the DR amplitude F_r we have to combine solutions like (112) to form an ingoing plane wave and then look at the outgoing waves. The total wavefunction will satisfy

$$\psi(\underline{k}_i) \to k_i^{-1/2}\exp(ik_iz)\zeta_iY_1 + F(\theta)\left(\frac{k_r}{M}\right)^{-1/2}\frac{e^{i\Omega}}{R}\Phi_r \tag{121}$$

where the asymptotic form of Φ_i is

$$\Phi_i \to \left(\frac{2k_i}{\pi}\right)^{1/2} J_{\ell_i}(k_ir)Y_1 + \text{outgoing waves}. \tag{122}$$

Expanding the plane wave in (121) into functions like (122) which connect to outgoing waves (118), we find that

$$F(\theta) = \frac{i\pi}{k_i}\sum_{\ell\lambda} A(\ell\lambda,\epsilon_i)i^{\ell}P_{\ell}(\cos\theta) \tag{123}$$

whence

$$\sigma_{DR}(\epsilon_i) = \frac{\pi}{k_i^2}\sum_{\ell\lambda}\left|2\pi A(\ell\lambda,\epsilon)\right|^2. \tag{124}$$

Usually a single value of $\ell\lambda$ predominates, e.g. the $1\sigma_u^2$ state of H_2 is coupled to a $d\sigma$ wave, $\ell\lambda = 2\sigma$.

The total cross section (124) thus depends on the matrix elements (118). Notice that the argument of V_{ri} is $\epsilon = \epsilon_i$, not ϵ_{ri}. Some idea of the cross section is obtained by inserting JWKB approximations to ζ_r, ζ_i in (118) and evaluating the integral by the method of stationary phase, with the result that[1]

$$\sigma_{DR} = \frac{4\pi^2}{k_i^2}\frac{\omega_e\, e^{-\rho}}{v(R_x)\left|W'_{ri}(R_x)\right|}\ ,\quad \rho = \int_{R_x}^{R_s}\frac{G_r\,dR}{v}. \tag{125}$$

The curves are supposed to cross at R_s, beyond which r is stable, $v(R)$ is the local velocity of the separating atoms, $W'_{ri} = (d/dR)(W_r-W_i)$, ω_e is the vibrational frequency of AB^+ and $R_x(\epsilon) < R_s$ is the point at which

$$W_r - W_i = \varepsilon. \tag{126}$$

The "survivel factor" $e^{-\rho}$ is the probability that AB^{**} does not autoionize between R_x and R_s. The reduced mass enters (125) only in $\rho \sim M^{1/2}$, so if $\rho \gg 1$ an isotope effect that σ_{DR} is larger for light species is expected. The semi-classical formula is only valid if R_s lies in the FC region of ζ_i. All too often R_s is on the edge of the FC region and a fully quantal description of the nuclear motion is required. In Fig. 9 we sketch the nuclear wavefunction squared $|\zeta_r(R)|^2$ at a given total energy. As ε increases, the classical turning point moves to smaller R, sweeping across the FC region. Thus below some pseudo-threshold σ_{DR} is small; then it rises rapidly varying with increasing ε as $|\zeta|^2$ varies with increasing R.

The general features just outlined are well illustrated by the case of H_2^+ for which experiments and detailed calculations are available. Figure 9 shows the potentials W_r, W_i and width G_r. We have plotted in Fig. 10 theoretical $\sigma_{DR}(v)$ against energy for H_2^+ initially in the v = 0, 1, and 2 vibrational states. The FC oscillations described in the preceding paragraph are clearly seen. The dip in $\sigma_{DR}(\varepsilon)$ at ε = 0.5 eV appears in recent experiments.[21] The cross section averaged over a known distribution of many initial vibrational states is compared with the measurements of Peart and Dolder[22] in Fig. 11. The cross section for producing H(n = 2) is also shown in Fig. 11. The distribution of final Rydberg states is predicted[13] over a wide range of energy and initial vibrational states to be

$$P(n) = 25.8\, n^{-3} \left[1 + \left(\frac{n_1}{n}\right)^4\right]^{-1} \tag{127}$$

where $n_1 = 4.5$, in harmony with the scant experimental evidence.[23] The final state atoms are not, as repeatedly stated without supporting arguments, concentrated in a single low-lying level (e.g. n = 2, 3), but are fairly evenly distributed over the levels n < 10. Within one level the population of each ℓ,m substate $\sim 1/(2\ell+1)$, since a Γ resonance can only couple to final states whose angular momentum projection on the internuclear axis is zero.

3.3. Very Low Energies: The Indirect Mechanism and Large Molecular Ions

At thermal energies (<< 1 eV) the matrix element A defined in (115) tends to a constant nonzero limit,

$$A(\ell\lambda,0) = \lim_{\varepsilon\to 0} \langle \zeta_r | V_{ri}(\varepsilon) | \zeta_i \rangle. \tag{128}$$

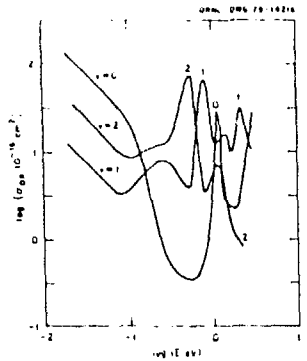

Fig. 10. Cross sections for DR of $H_2^+(v)$ as a function of impact energy.

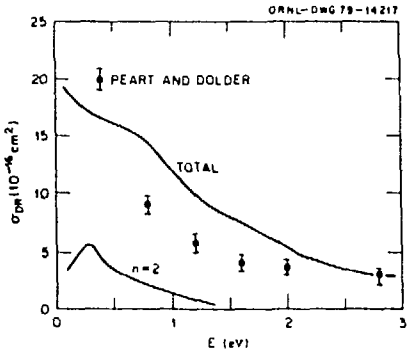

Fig. 11. Cross sections for DR of H_2^+(all v) → H + H(n) as a function of impact energy. Total (all n) compared with experiment,[22] H(n = 2) contribution also shown.

This limit is a consequence of the long-range Coulomb attraction between the ion and electron. Then the cross section (124) becomes

$$\sigma_{DR} = \frac{2\pi^2 G}{k_i^2}, \quad G = 2\pi|A(\ell\lambda,o)|^2. \tag{129}$$

The same form follows from the semiclassical approximation (125) since $R_x \to R_s$ as $\varepsilon \to \infty$. From (129) we get the well-known rate

$$\alpha_{DR} = \frac{(2\pi)^{3/2}}{T^{1/2}} G = (1.717 \times 10^{-10}\ \text{cm}^3\ \text{sec}^{-1}) \frac{G\ \text{degK}}{(T\ \text{degK})^{1/2}}. \tag{130}$$

Since G ~ 2 eV for a broad molecular resonance, $\alpha_{DR} \sim 2 \times 10^{-7}$ $\text{cm}^3\ \text{sec}^{-1}$ at 400 degK, as observed in many species.[20]

The form of (130) is more fundamental than is often supposed as we can see by developing a classical model.[24] Suppose the electron approaches the ion on a trajectory defined by the initial kinetic energy $\varepsilon_i = k_i^2/2$ and impact parameter b; the distance of closest approach is r, the velocity there being v. We assume that within $r < r_o$ recombination takes place with probability P_R. The electron will almost always lose kinetic energy $\Delta\varepsilon$ and angular momentum Δj to the ion, especially to a large ion. The conservation of energy and angular momentum require

$$k_i b = vr + \Delta j \tag{131}$$

$$k_i^2 = v^2 + 2\Delta\varepsilon - 2/r \tag{132}$$

whence recombination is possible if $b < b_o$ given by

$$k_i b_o = \Delta j + (2r_o)^{1/2} [1 + r_o(\varepsilon_i - \Delta\varepsilon)]^{1/2}. \tag{133}$$

We are only interested in $\varepsilon_i \ll 1$ eV while $r_o < 4$ for even the largest ionic cluster, so the square brackets in (133) can be replaced by unity, leading to a cross section

$$\sigma_{DR} = \frac{\pi P_R}{k_i^2} \sum P_T(\Delta j)[\Delta j + (2r_o)^{1/2}]^2. \tag{134}$$

The probability of angular momentum transfer Δj is denoted by $P_T(\Delta j)$, while the sum is over all $\Delta j > -(2r_o)^{1/2}$. If P_T is ~ 1 for $\Delta j \geq 1$, and $r_o \sim 2$, (134) is consistent with (129) if $9P_R \sim 2\pi G$, i.e. $P_R \sim 0.04$. Thus, unless $\Delta j \gg 1$, a situation discussed below, the temperature dependence (130) is inescapable.

In the *indirect* mechanism of DR, first discussed in detail by Bardsley, the electron gives up its energy in vibrational excitation, settling in a Rydberg state until dissociation or reverse ionization takes place,

$$e(k_i\ell_i\lambda_i) + AB^+(v_i) \rightleftarrows [e(n\ell_s\lambda_s)AB^+(v_s)] \to AB^{**} \to A+B. \tag{135}$$

Rotational excitation is possible but does not seem to be of practical importance. The theory of (135) is similar to that of DIR.[19] The indirect rate is of the form (130) with G replaced by a sum like (75),

$$G_{IDR} = \pi^{-1} \sum_{s,n} \frac{\Gamma_d(s,n)\Gamma_a(s,n)}{\Gamma_d(s,n) + \Gamma_a(s,n)} \exp\left[-\frac{\varepsilon(s,n)}{T}\right]. \tag{136}$$

Relative to the initial state, the resonance energies are given by

$$\varepsilon(s,n) = U_{si} - \frac{1}{2n^2}. \tag{137}$$

The dissociation width Γ_d is analogous to Γ_r in (75), except that it depends on n,

$$\Gamma(s,n) = n^{-3}\, G(v_s). \tag{138}$$

The present autoionization width Γ_a is entirely analogous to the earlier Γ_a, and can be related to the threshold vibrational excitation cross section in the manner of (77),

$$\Gamma(s,n) = n^{-3}\, G_{ex}(v_s) \tag{139a}$$

$$\sigma_{ex}(v_i \to v_s) = \frac{\pi}{k_i^2} G_{ex}(v_s) \tag{139b}$$

Inserting (139) and (139) in (136), each term varies as n^{-3}. The sum over n can be done analytically so that

$$G_{IDR} = \sum_s \frac{G(v_s)G_{ex}(v_s)}{G(v_s) + G_{ex}(v_s)} \left[1 - \exp\left(-\frac{U_{si}}{T}\right)\right]. \tag{140}$$

Early discussions of DR fell down, like early discussions of DIR, in not summing over an entire Rydberg series; thus, they incorrectly found that as $T \to 0$, $G \sim T^{-1}$, a result which is still quoted. If $G \gg G_{ex}$,

$$G_{IDR} = \sum G_{ex}(v_s) \quad , \quad \alpha_{IDR} = \alpha_{TX}, \tag{141}$$

the total rate for vibrational excitation, which *ex hypothesi* $\ll \alpha_{DR}$. However, if $G_{ex} \gg G$ (independent of v_s),

$$G_{IDR} = NG, \quad \alpha = (1 + N)\alpha_{DR} \tag{142}$$

where N is the number of levels s for which $G_{ex}(v_s) \gg G$, $U_{si} \geq T$. Thus in a diatomic α_{DR} is usually multiplied by two; this factor has been included in the cross sections in Fig. 10 below 0.1 eV. In polyatomic ions N may be very large[24] e.g. in clusters $Y^+ \cdot X_n$, $N \sim n$. However, (140) still predicts a rate $\sim T^{-c}$, $c \geq \frac{1}{2}$.

Recent experiments of Biondi[25] strongly suggest that $\alpha_{DR} \sim T^0$ for large clusters. In the regime where Δj is small (c.f. (131) - (134)) no reasonable assumption will lead to such a variation since neither r_0 nor P_R can $\sim T$. Nor can we postulate that $G_{ex} \sim k_1$ (which is in any case impossible) since if $\alpha_{IDR} \sim G_{ex}$, $\alpha_{DR} \gg \alpha_{IDR}$, as explained above. However, a large cluster with rotational constants $B \sim 10^{-7}$ can absorb a great deal of angular momentum from the incident electron. For a cluster $Y^+ \cdot X_n$ of internal energy E_R, the mean vibrational dipole moment[24]

$$\mu = \frac{K\rho_e}{\omega_e}\left(\frac{\hbar E_R}{n}\right)^{1/2} \tag{143}$$

where $K \sim 1$ and ρ_e, ω_e are the length and frequency of an XY^+ bond. Since $B \sim n^{-1}$, μ should vary little with n. At an impact parameter b_0, the electron dipole interaction can couple states within a band of quantum numbers Δj such that

$$\Delta E_R = 2(B E_R)^{1/2} \Delta j = \frac{\mu}{b_0^2}. \tag{144}$$

Inserting (144) in (133) and assuming that $\Delta j \gg (2r_c)^{1/2}$, i.e., that the electron loses most of its angular momentum, we obtain

$$\alpha_{DR} = \frac{\pi P_R b^{2/3}}{(8\hbar E_R \varepsilon_i)^{1/3}} = \frac{\pi P_R}{(n\varepsilon_i)^{1/3}}\left(\frac{K\rho_e}{\omega_e}\right)^{2/3}. \tag{145}$$

We must emphasize that this is *not* indirect DR since $\Delta E_R \sim 0.01\ \varepsilon_i$ only. If P_R is the probability of exciting a vibrational mode which $\sim n$,

$$\alpha_{DR} \sim n^{2/3} T^{1/6}, \tag{146}$$

fairly close to the observed behavior $\sim nT^0$. Trying some numerical values, (145) gives a maximum $\alpha_{DR} \sim 10^{-7}$ in accord with the observed rates for large clusters $\sim 10^{-5}$ cm^3 sec^{-1}. For T = 5000 deg K, E_R = 400 deg K, (144) gives $b_0 \sim 100$, $\Delta j \sim k_1 b_0 \sim 10$, $\Delta E_R \sim 6$ deg K so that the model is internally consistent.

3.4. Other Topics

The reader is referred to review articles[20,26] and recent papers[27] for more information. A number of theoretical studies have been made of CH_3^+; while the potentials are fairly well understood, the dynamics of the process are not. The crossing state is the fourth state of $^2\Pi$ symmetry so that a series of curve-hopping transitions are needed to reach the final dissociation products. Such mechanisms are presumably common in atmospheric and astrophysical species and merit investigation. We have already mentioned the difficulty of dissociating H_3^+ from the ground vibrational state at thermal energies. All extant measurements on H_3^+ have used unrelaxed ions (internal energy 2-4 eV) produced by the $H_2^+ + H_2$ reaction. While these experiments are mutually consistent they say nothing about the ground state ion. As far as experimental techniques go, the greatest obstacle to progress is the incapacity to select the initial vibrational state.

§ 4. THREE-BODY RECOMBINATION

4.1. Introduction

We now turn to three-body (or to be erudite, ternary) processes which dominate at high densities. The rate of such a process as (3) is described by a quantity β of dimension L^6T^{-1} such that

$$\frac{dn(x^+)}{dt} = \frac{dn(y^-)}{dt} = -\beta n(x^+)n(y^-)n(z). \tag{147}$$

We can equivalently use an effective ternary rate

$$\alpha_{TR} = n(z)\beta. \tag{148}$$

Many three-body reactions are of great practical importance, e.g. recombination in air,

$$O_{2m}^{+} + O_{2n}^{-} + (N_2,O_2) \rightarrow (m+n)O_2 + (N_2,O_2) \qquad (149)$$

where $m,n < 4$. But we begin with the electronic process $y^{-} + z \rightarrow e$ which, e.g., predominates in a helium afterglow $X = He$,

$$e + e + X^{+} \rightarrow e + X(p). \qquad (150)$$

4.2. Electronic Three-Body Recombination

To arrive at a "rate" for (150), one must consider all the processes illustrated in Fig. 12. The quantity one really wants to know is the net increase in ground state neutral atoms per unit time. We first describe the rate equation approach of Bates *et al.*[28,29] A plasma is considered with predominantly singly charged ions X^{+}. The number density of free electrons is $n(^{e})$ and of neutrals in the Rydberg level p is n(p), all number densities being scaled to $n(X^{+}) = 1$. We suppose (call this assumption A-1) that the free electrons are in Saha equilibrium and that all rates can be averaged accordingly. The processes considered in an optically thin medium, with their rate coefficients, are as follows:

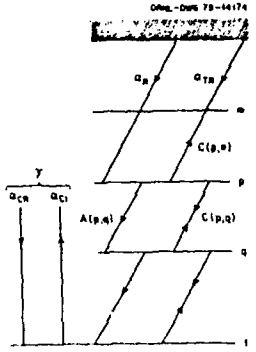

Fig. 12. Scheme of electronic three-body recombination: quantities occurring in (152).

(i) radiative recombination $\alpha_R(p)$,

(ii) spontaneous emission $A(p,q)$, $p > q$,

(iii) collisional excitation and de-excitation, $C(p,q)$,

(iv) collisional ionization $C(p,^{e})$ and its inverse, ternery recombination.

The last-mentioned rate can be written as in (148),

$$C(^{e},p) = \beta(p)n(^{e}) = \alpha_{TR}(p). \qquad (151)$$

The rate equation governing the relaxation of n(p) is

$$\frac{dn(p)}{dt} = n(^{e})[\alpha_R(p) + n(^{e})\beta(p)] + \sum n(q)[C(q,p) + A(q,p)] - n(p)[\tilde{C}(p) + \tilde{A}(p)] \qquad (152)$$

$$\tilde{C}(p) = C(p,^{e}) + \sum C(p,q) \quad , \quad \tilde{A}(p) = \sum A(p,q). \qquad (153)$$

We make a second assumption (A-2) that levels $p \geq 2$ are in a steady state

$$\frac{dn(p)}{dt} = 0 \quad , \quad p \geq 2. \qquad (154)$$

If p_{max} levels are explicitly considered, and those with $p > p_{max}$ are in Saha equilibrium (A-3), (154) provides $p_{max}-1$ equations for $n(2) \ldots n(p_{max})$ whose solution is written

$$n(p) = R(p) + n(^{e})R_e(p). \qquad (155)$$

Substituting (155) in (152) for p = 1, we find that

$$\frac{dn(1)}{dt} = -\gamma n(^{e})n(1) \quad , \quad \gamma = \alpha_{CR} - \alpha_{CI}n(1)/n(^{e}) \qquad (156)$$

where γ is a ground recombination coefficient, made up of collisional-radiative and collisional-ionization parts, given by

$$\alpha_{CR} = \alpha_R(1) + \beta(1)n(^{e}) + \sum R_e(q)[C(q,1) + A(q,1)] \qquad (157)$$

$$\alpha_{CI} = \tilde{C}(1) - \sum R(q)[C(q,1) + A(q,1)]. \qquad (158)$$

The meaning of each term in (157)-(158) is readily grasped.

At low $n(*)$, roughly $< 400\ (T \text{ deg K})^2$, $\alpha_{CR} = \alpha_R(1)$. In the other limit one reaches a purely collisional regime where

$$\gamma = \alpha_{CR}^{-} = \beta^{-} n(*). \tag{159}$$

The solutions at moderate and high densities are largely determined by the choice of $\beta(p)$ and $C(p,*)$. Bates *et al.*[28] used binary encounter expressions. The energy transfer cross section for $e(\varepsilon) + e'(\varepsilon') \rightarrow e(\varepsilon-U) + e'$ is

$$\sigma(\varepsilon,U)dU = \frac{4\pi}{c}\frac{dU}{U^2}. \tag{160}$$

For ionization of a state with binding energy U_p, (160) leads to the cross section

$$\sigma_{BEI}(p) = \frac{2\pi}{U_p c} \tag{161}$$

and the rate

$$C(p,*) = \frac{(2\pi)^{1/2}}{U_p T^{1/2}}. \tag{162}$$

The condition for recombination into p is that U lies between $\varepsilon' + U_p$, $\varepsilon' + U_{p-1}$, while e is within the radius of the p state. The cross section for e fixed is

$$\sigma_{BRR}(\varepsilon' \rightarrow p) = \frac{4\pi}{\varepsilon}\frac{(2U_p)^{3/2}}{(\varepsilon'+U_p)^2}. \tag{163}$$

To get a ternery rate, one must integrate over the velocity distributions of e,e', the impact parameters of e (already done in (163)) and the configuration space of e', to obtain,

$$\beta(p) = \frac{4\pi^{3/2}}{U_p^{3/2}\, T^{1/2}(T+U_p)^2}. \tag{164}$$

Summing (164) over p such that $U_p \geq T$, i.e. over levels which are unlikely to be re-ionized, we arrive at an estimate of γ,

$$\gamma_{BE} \approx \frac{0.98}{T^{9/2}} \tag{165}$$

which is surprisingly close to the results of elaborate calculations. Numerical results will be discussed after considering the alternative approach of Keck *et al.*[30]

This second approach is closer to the spirit of statistical mechanics. The process by which a given electron trickles down the ladder of excited states into the ground state while interacting with the third-body electron is treated as a single dynamical process. Then the rate is found by averaging over a ternery hypercross-section. A very simple argument of this type was used to derive (164) and (165). The ternary approximation should be valid for densities $< 10^{19}$ cm^{-3}.

The earliest statistical model[31] was that of J. J. Thomson who introduced a characteristic energy and associated Bohr radius,

$$E_T = \tau T \quad , \quad r_T = E_T^{-1} \tag{166}$$

where $\tau \sim 1$ (the original guess was $\tau = 3/2$). Electrons which acquire more potential energy than E_T, i.e. which come within r_T of the nucleus, are unlikely to be knocked back into the continuum. Thomson further assumed that if two electrons come within the sphere $r < r_T$, one is likely to be stabilized. The rate

$$\gamma = K \langle v r_T^5 \rangle = 1.73\ K\ T^{-5}\ T^{-9/2} \tag{167}$$

where $K \sim 1$. A more precise derivation was developed by Keck[30] from Wigner's formulation of chemical transition state theory. He argued that the rate is exactly given by

$$\gamma = \int n\, v_n (1-Q) dS \tag{168}$$

where S is an eleven-dimensional hypersurface in the phase space of the two electrons, dividing the region of two free electrons from that of one bound electron; n is the number density, v_n the velocity normal to S and Q the probability that the trajectory crossing S at a given point later doubles back across S. An upper bound (the "variational estimate" γ_{Var}) is obtained if $Q = 0$. Thomson's criteria provide a good choice of surface

$$H_1 = -E_T \quad , \quad H_2 \geq -E_T \tag{169}$$

where H_1, H_2 are the total energies of the recombinant and spectator electrons. As so defined γ_{Var} diverges as $r_2 \rightarrow \infty$. However, very distant electrons do not transfer energy on average[†] if the

[†]This is not a quantal condition. Mansbach and Keck[30] point out that the same criterion is required in stellar dynamics.

interaction time r_2/v_2 times the classical orbital frequency exceeds a number δ - 1, i.e. unless

$$\frac{r_2}{r_T} < \delta\tau^{1/2}. \tag{170}$$

The resulting

$$\gamma_{Var} = 0.470\ T^{1/2}\ r_T^5\ f(\tau),\ f(\tau) = \delta^2\ \tau e^{\tau}(1+8e^{3\tau/5}) \tag{171}$$

where $\tau^{-5} f(\tau)$ has a minimum value $11.5\delta^2$ at $\tau = 2.52$. Thus the best estimate is

$$\gamma_{opt} = 5.40\delta^2\ T^{-9/2} = \frac{(2.44 \times 10^{-8}\ cm^3\ sec^{-1})\delta^2}{(T\ deg\ K)^{9/2}}. \tag{172}$$

The optimum surface is often called the "bottleneck".

To obtain a better estimate, Mansbach and Keck sampled trajectories starting on S to see what fraction doubled back. With a choice of $\delta = 1/2$, this fraction Q = 0.36 so that

$$\gamma_{MCarlo} = 0.67\ T^{-9/2} = \frac{2.0 \times 10^{-8}\ cm^3 sec^{-1}}{(T\ deg\ K)^{9/2}} \tag{173}$$

which is close to (165). In Fig. 13 we plot β^{-} (c.f. (159)) from Bates *et al.*[28,29] against temperature for comparison with γ_{MCarlo}. The agreement is remarkable. The rate equation approach selects the important physical processes, viz. those with fairly large energy transfers, which are not sensitive to the cutoff (170). Hence no such adjustable parameters are required.

4.3. Ionic Three-Body Recombination

We now consider processes of type (3) where x^+, y^- are ions and z = neutral,

$$X^+ + Y^- + Z \rightarrow [X^+Y^-] + Z \rightarrow XY + Z. \tag{174}$$

Harking back to the Thomson model, we suppose that X^+, Y^- must first approach within r_T and then one or the other has to collide with a Z to stabilize the complex $[X^+Y^-]$. The final step, whose details do not affect the rate, is usually that $[X^+Y^-]$ undergoes a curve crossing transition to a covalent state XY, either bound or

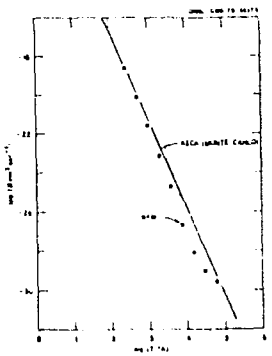

Fig. 13. β^{-} calculated by Bates, Kingston, and McWhirter[28,29] compared with γ_{MCarlo} calculated by Mansbach and Keck[30] as functions of temperature.

dissociating. The crossing separation is typically - 5 a_o corresponding to a Coulomb potential energy - 5 eV. The collision probability is determined by the $X + Z$, $Y^- + Z$ diffusion cross sections, denoted by σ_X, σ_Y. If Z has a dipole polarizability P_Z, the gas kinetic cross sections are closely given by the Langevin model

$$\sigma_X,\ \sigma_Y = \pi \left(\frac{P_Z}{T}\right)^{1/2}. \tag{175}$$

A typical collision radius - 10 a_o << r_T - 10^3 a_o. The probability of a collision within the Thomson sphere is[31,32]

$$Q = \frac{4}{3} r_T\ (L_X^{-1} + L_Y^{-1}),\ L_X^{-1} = n(Z)\sigma_X,\ \text{etc.} \tag{176}$$

where L_X, L_Y are mean free paths for X,Y in Z. The ternery recombination rate is

$$\beta = \frac{\pi r_T^2}{n(Z)} \langle v_{XY} \rangle = \frac{4\pi}{(3M_{XY})^{1/2}} \cdot \frac{(\sigma_X + \sigma_Y)}{T^{5/2}} \tag{177}$$

where M_{XY} is a reduced mass; r_T and τ were defined by (166). From (175), $\beta \sim T^{-3}$. Although the steep dependence on τ is disturbing, (177) is easy to apply.

The approach of Bates and his collaborators[31,32] is analogous to that used in the electron problem. Rate equations similar to (152) are set up (radiative processes are insignificant here) and solved. The Rydberg states p are now so close together that they might as well be treated as continuous. We have to introduce three semi-arbitrary negative energies:

(i) E_c ($> T$) is analogous to p_{max} in defining the edge of the continuum. Higher levels are in Saha equilibrium.

(ii) E_d ($< T$) is the level above which populations are stationary, analogously to p = 2 earlier.

(iii) E_s ($< E_d$) is the stabilization level at which X^+,Y^- neutralize by charge transfer. As stated above, $-E_s \sim 5$ eV.

The equations analogous to (154) are

$$n_i \int_{E_d}^{\infty} C_{if}\, dE_f = \int_{E_s}^{\infty} n_f C_{if}\, dE_f \qquad (178)$$

where the kernel $C_{if} = C(E_i \to E_f)$ gives the rate of energy transfer to $X^+ + Y^-$ by collisions with Z; as before C_{if} is calculated in the binary encounter model. Once (178) has been solved for n(E), E $> E_d$, the recombination rate

$$\beta = \left\langle \int_{E_d}^{E_o} (n_i - n_f) C_{if}\, dE_f \right\rangle \qquad (179)$$

where the triangular brackets denote a Maxwellian average over E_i. Rate coefficients have been extensively tabulated as functions of the mass ratios and ion-neutral cross sections.[31,32]

Bates and Flannery have assessed the validity of the Thomson model.[32] In Fig. 14 we show their calculation of the probability $P(\tau)$ that a system which reaches $E = -\tau T$ does *not* return to the continuum. As $\tau \to 0$, $P \to 0$ rapidly, but $P \to 1$ when $\tau > 2$. For equal masses (177) is very accurate if $\tau = 1.89$. The results of calculations by Bates and Flannery[32] on $O_4^+ + O_2^-$, $O_4^+ + O_4^-$ and $O_4^- + O_2$ are compared in Fig. 15 with recent experiments[33] at densities below

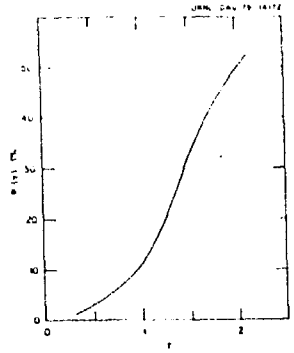

Fig. 14. Probability that a system which reaches $-\tau T$ does not return to the continuum.[32] Parameters (c.f. (177)) are T = 400 deg K, $\sigma_X = \sigma_Y = 4 \times 10^{-14}$ cm^2, $M_X = M_Y = 1.17\, M_Z$.

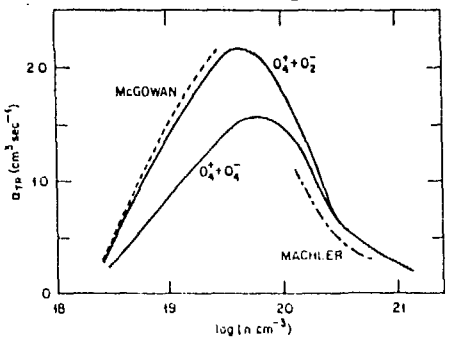

Fig. 15. Recombination in oxygen over a wide range of densities. At $n < 3 \times 10^{19}$ cm^{-3} the Bates-Flannery theory[32] for two mechanisms is compared with the measurements of McGowan.[33] At higher densities the transition to Langevin theory is described by a semi-empirical prescription and compared with the measurements of Mächler on air.[34]

$n = 3 \times 10^{19}$ cm^3. The former mechanism is theoretically favored.

At densities $n > 3 \times 10^{19}$ cm^{-3} the assumption of ternery collisions breaks down. At very high densities $n > 3 \times 10^{20}$ cm^{-3} recombination is described by a theory due to Langevin. He considered the ions diffusing towards each other under the influence of their Coulomb attraction. If the ionic mobilities of X^+, Y^- in Z are K_+, K_-, the mean velocity of approach at a distance r is

$$v_d = \frac{Ke}{r^2}, \quad K = K_+ + K_- \text{ (c.g.s. units)}. \tag{180}$$

Then the effective two-body recombination coefficient is

$$\alpha_{TR} = 4\pi r^2 v_d = 4\pi Ke \quad \text{(c.g.s. units)}. \tag{181}$$

Thus $\alpha_{TR} \sim [n(Z)(\sigma_X + \sigma_Y)]^{-1}$ instead of $[\ldots]^{+1}$ as at low densities. Many semi-empirical prescriptions have been suggested for joining (177) to (181) at intermediate densities, none very satisfactory. In Fig. 15 such a theory has been used at high densities, i.e. beyond the linear régime, and compared with very old experiments on air.[34] A true unified theory, valid at all densities, would be a considerable achievement.

References

1. D. R. BATES and A. DALGARNO (1962) in "Atomic and Molecular Processes" (ed. D. R. Bates) p. 245, Academic Press, New York.

2. H. A. BETHE and E. E. SALPETER (1957) "Quantum Mechanics of One- and Two-electron Atoms", Springer, Berlin.

3. L. D. LANDAU and E. M. LIFSHITZ (1971) "Classical Theory of Fields", p. 181, Pergamon Press, New York.

4. M. ABRAMOWITZ and I. A. STEGUN (1964) "Handbook of Mathematical Functions", NBS, Washington.

5. G. N. WATSON (1966) "Treatise on the Theory of Bessel Functions", University Press, Cambridge.

6. D. H. MENZEL and C. L. PEKERIS (1935) MNRAS 96, 77.

7. R. W. DITCHBURN and U. OPIK (1962) in "Atomic and Molecular Processes" (ed. D. R. Bates) p. 79, Academic Press, New York.

8. L. SPITZER (1968) "Diffuse Matter in Space", p. 117, Interscience, New York.

9. A. BURGESS (1958) MNRAS 118, 477.

10. D. R. BATES (1961) "Quantum Theory I. Elements", Academic Press, New York; N. F. MOTT and H. S. W. MASSEY (1966) "Theory of Atomic Collisions", University Press, Oxford.

11. A. BURGESS (1965) 141, 1588; (1964) 139, 776; (1960) Ap. J. 132, 503.

12. B. SHORE (1969) Ap. J. 158, 1205.

13. R. GAYET, D. HOANG BINH, F. JOLY, and R. McCARROLL (1969) Astron. and Astrophys. 1, 365.

14. M. J. SEATON and P. J. STOREY (1976) in "Atomic Processes and Applications", p. 133 (ed. P. G. Burke and B. L. Moiseiwitsch) North-Holland, Amsterdam.

15. M. SUTER, C. B. VAHR, E. B. HINTON, J. D. ALTON, P. M. GRIFFIN, R. S. THOE, L. WILLIAMS, and I. A. SELLIN (1979) Z. f. Physik A289, 433.

16. G. A. MARTIN and W. L. WIESE (1976) J. Phys. Chem. Ref. Data 5, 565.

17. J. WEISHEIT (1975) J. Phys. B 8, 2556.

18. J. DUBAU (1973) Ph.D. Thesis, University of London.

19. C. BOTTCHER (1976) J. Phys. B 9, 2899; (1974) Proc. Roy. Soc. A340, 361.

20. J. N. BARDSLEY and M. A. BIONDI (1970) Adv. Atom. Molec. Phys. 6, 1.

21. D. AUERBACH, R. CACAK, R. CAUBANO, T. D. GAILY, C. J. KEYSER, J. Wm. McGOWAN, J. B. A. MITCHELL, and S. F. J. WILK (1977) J. Phys. B 10, 3797.

22. B. PEART and K. T. DOLDER (1973) J. Phys. B 6, 2409; (1973) 6, L359; (1974) 7, 236.

23. R. A. PHANEUF, D. H. CRANDALL, and G. H. DUNN (1975) Phys. Rev A11, 528.

24. C. BOTTCHER (1978) J. Phys. B 11, 3887; B. M. SMIRNOV (1977) Sov. Phys. - Usp. 20, 119.

25. C. M. HUANG, M. WHITAKER, M. A. BIONDI, and R. JOHNSEN (1978) Phys. Rev. A18, 64; C. M. HUANG, M. A. BIONDI, and R. JOHNSEN (1976) Phys. Rev. 14, 984; M. T. LEU, M. A. BIONDI, and R. JOHNSEN (1973) Phys. Rev. A7, 292; A8, 413

26. K. T. DOLDER and B. PEART (1976) Rep. Prog. Phys. 39, 693.

27. J. Wm. McGOWAN, P. M. MUL, V. S. D'ANGELO, J. B. A. MITCHELL, P. DEFRANCE, and H. R. FROELICH (1979) Phys. Rev. Letts. 42, 373; J. B. A. MITCHELL and J. Wm. McGOWAN (1978) Ap. J. Letts. 222, 77; R. D. DUBOIS, J. B. JEFFRIES, and G. H. DUNN (1978) Phys. Rev. A17, 1314; F. L. WALLS and G. H. DUNN (1974) J. Geophys. Res. 79, 1911.

28. D. R. BATES, A. E. KINGSTON, and R. P. W. McWHIRTER (1962) Proc. Roy. Soc. A267, 297.

29. E. W. McDANIEL (1964) "Collision Phenomena in Ionized Gases", John Wiley, New York.

30. J. C. KECK (1972) Adv. At. Molec. Phys. 8, 39; P. MANSBACH and J. C. KECK (1969) Phys. Rev. 181, 275; B. MAKIN and J. C. KECK (1964) in "Atomic Collision Processes", p. 510 (ed. M. R. C. McDowell) North-Holland, Amsterdam.

31. M. R. FLANNERY (1972) Case Studies in Atomic Collision Physics 2, 1.

32. M. R. FLANNERY (1976) in "Atomic Processes and Applications", p. 407 (ed. P. G. Burke and B. L. Moiseiwitsch) Academic Press, New York; D. R. BATES and H. J. MOFFETT (1966) Proc. Roy. Soc. A291, 1.

33. S. McGOWAN (1967) Can. J. Phys. 45, 439.

34. W. MACHLER (1976) Z. Phys. 134, 1.